Real-Time Prediction of Fish Cage Behaviors under Varying Currents using Deep Neural Network

Sihan Gao[1], Peihua Han[2], Lars Christian Gansel[1], Guoyuan Li[2] and Houxiang Zhang[2]

***Abstract*— This paper presents a Deep Neural Network (DNN) model for rapid and low-cost prediction of fish cage behavior under varying currents. We employ a numerical model of the fish cage created in Orcaflex and a set of current profiles from the water surface to the bottom of the cage (0-30 m). A DNN model is trained on a subset of simulated results and evaluated on a separate dataset. Our findings demonstrate that the DNN model can provide real-time, model-free predictions of fish cage behavior comparable to those of the simulator, with improved computational efficiency and robustness. The method is demonstrated to be suitable for digital twin applications, offering near-instant updates on cage behavior and valuable insights for ensuring the safety and stability of fish cage structures in challenging ocean environments.**

I. INTRODUCTION

Sea-based salmon farming is an essential part of the global seafood industry. Open net cages are the most common facilities applied to stock salmon, especially in Fjord environments, as an example shown in Fig. 1. The cages, mainly consisting of flexible structures, can experience significant deformation caused by variations in current velocities over both space and time. Such changes in cage shapes can affect the safety, productivity, and sustainability of salmonid farming.

The current patterns in a fjord can be influenced by a combination of factors, including tides, freshwater inflow, wind-driven currents. Tidal currents are one of the most significant drivers of flow patterns in a fjord. As the tide rises and falls, water flows in and out of the fjord, creating strong currents that can move in different directions depending on the topography of the fjord. Freshwater inflows from rivers or glaciers can also impact flow patterns in a fjord, creating low salinity areas. In addition, wind-driven currents can create variable flow patterns that can interact with tidal currents and freshwater inflows.

Various technologies have been developed to accurately measure the current velocity at fish farms, with Acoustic Doppler Current Profiler (ADCP), Electromagnetic Current Meter (EMCM), and Satellite Imagery being some of the most commonly used ones. Among these, ADCP stands out as the technology most widely applied in the aquaculture industry. ADCP works by emitting sound waves in three or four beams that reflect off particles present in the water and subsequently measure the frequency shift of the sound waves as they return to the instrument. This frequency shift, caused by the Doppler effect, enables the ADCP to calculate the speed and direction of the currents with high resolution along its beams. In practical terms, ADCPs are deployed in close proximity to aquaculture structures, where they continuously measure the incoming current profile over a specified time interval (typically 5 or 10 minutes) and transmit this information remotely for monitoring purposes.

Fig. 1: A fish farm in Storfjord in Norway.

The prediction of fish cage behavior under varying current conditions can be accomplished through the use of numerous numerical cage models. For instance, [1], [2] have proposed models for this purpose. Additionally, [3] utilized Computational Fluid Dynamics (CFD) technology to develop a Structure Fluid Interaction (SFI) model, which was effective in analyzing the behaviors of fish cages exposed to incoming flows and its ambient flow field. Although these models rely on certain simplifications to reduce computational costs, they are predominantly employed in net cage research and design, and therefore, simulation time is not a primary concern. The time required for a single current case simulation can range from minutes to hours, depending on the complexity of the model. Notably, the resolution of current input significantly impacts the accuracy of predictions. [4] indicate the vertical variability of current velocity in some fish farms, where an averaged current velocity can lead to substantial errors due to drag forces proportional to the square of flow velocity. It is, therefore, imperative to consider the resolution of current input to enhance the quality of predictions.

[1] S. Gao and L. C. Gansel are with Department of Biological Sciences Ålesund, Norwegian University of Science and Technology, Ålesund 6009, Norway {Sihan.gao, lars.gansel}@ntnu.no

[2] P. Han, G. Li, and H. Zhang are with Department of Ocean Operations and Civil Engineering, Norwegian University of Science and Technology, Ålesund 6009, Norway {peihua.han, guoyuan.li, hozh}@ntnu.no

The recent advancement in digital technologies has made it possible to create a digital prototype of fish cages to the monitoring of their behavior under varying flows. A digital prototype is a virtual representation of a physical object or system driven by a physical engine or data-driven method, allowing for testing and real-time system performance monitoring. [5] Authors of [6] proposed a simulator based on a simplified net structure model for monitoring the interactions of stocked fish and cages. [7] applied digital prototypes of fish cages in a simulation center for training fish farming staff. [8], [9] integrated sensor data with cage simulation results. In these previous works, the digital fish cages are driven by numerical models based on physics; therefore, a simulator keeps running is necessary. In other fields [10], creating a data-driven model can be a good solution to achieve quick, robust and low-cost prediction.

In this paper, we applied Deep Neural Network (DNN) for quick and low-cost predictions of fish cage behaviors under varying currents. The current flow velocities there show apparent variation in the depth direction, likely caused by the interactions of tidal currents, wind currents, and seabed topology. Our method employs a numerical model of the fish cage created in the dynamic analysis software Orcaflex, and a set of current profiles from the water surface to the bottom of the cage (0 – 30 m) are defined. Our results show that the proposed method can achieve real-time, model-free predictions of fish cage behavior, making it suitable for digital twin applications.

II. Establishment of DNN model for fish cage behavior prediction

A. Framework

The study employs a set of current profiles that mimic possible incoming currents at fish farms. The current information was input into a simulator to generate corresponding cage behaviors, including the shape of the cage and mooring forces. Part of the simulated results, along with their current conditions, was used as a subset to train a DNN model. The trained DNN model was then evaluated using the remaining dataset by comparing the model's predictions with the simulated results. (Fig. 2)

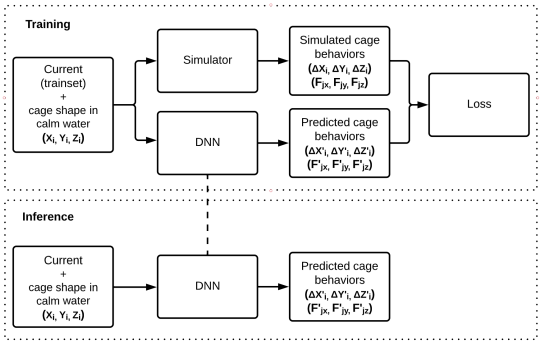

Fig. 2: Schematic of establishing the DNN model.

TABLE I: Configurations of the net cage as the prototype

Cage Dimension	
Diameter [m]	39.2
Depth of cylindrical net [m]	15.0
Depth of conical net [m]	12.0
Netting configurations	
Nominal bar length [mm]	18.00
Twine thickness [mm]	1.89
Floating ring	
Diameter [m]	41.0
Pipe Diameter [cm]	35.0
Pipe Thickness [cm]	3.0
Pipe Material	HDPE
Sink ring	
Diameter [m]	42.0
Pipe Diameter [cm]	35.0
Pipe Thickness [cm]	3.0
Pipe Material	HDPE
Submerge weight [Kg/m]	50.0
Bottom weight	
Submerge weight [Kg]	200
Mooring line	
length [m]	8*45.0
Rope diameter [cm]	10.0

A set of predefined current conditions was established based on the following rules: 1) The current profiler was designed with six layers evenly distributed from the water surface to a depth of 30 m, with the current speed being constant within each layer. 2) The magnitude of the surface current was randomly generated from a range of 0.15 to 0.7 m/s, and its direction was randomly derived from -30 to 30 degrees. 3) The current velocity of the following layer deviated from its upper layer with a ±15% variation in current speed and ±15 degrees in the current direction. These parameters were chosen to simulate realistic current conditions and to provide a suitable training base for the experiment.

In total, 390 current cases were established and input into a simulator. The corresponding cage behavior, including the deformations of the net, floating ring, and sink ring, as well as the forces at the four mooring buoys, were extracted. The current conditions, combined with their corresponding cage behavior, were then used to establish a Deep Neural Network (DNN) model. Of the 390 cases, 300 were utilized for model training purposes, while the remaining cases were reserved for model evaluation.

B. Modeling of the cage structures in Orcaflex

The behavior of a net cage subject to various current conditions was simulated using a generic dynamic analysis software called OrcaFlex, commonly used to simulate the behavior of marine systems such as floating structures, moorings, and umbilical. The configurations of the prototype cage are shown in Table I.

The net structure was modeled using several truss elements to optimize computational costs. Each truss element represented the parallel strands of the physical net. The fan-shaped sections on the conical bottom of the cage were modeled using one radial and one circumferential truss element each,

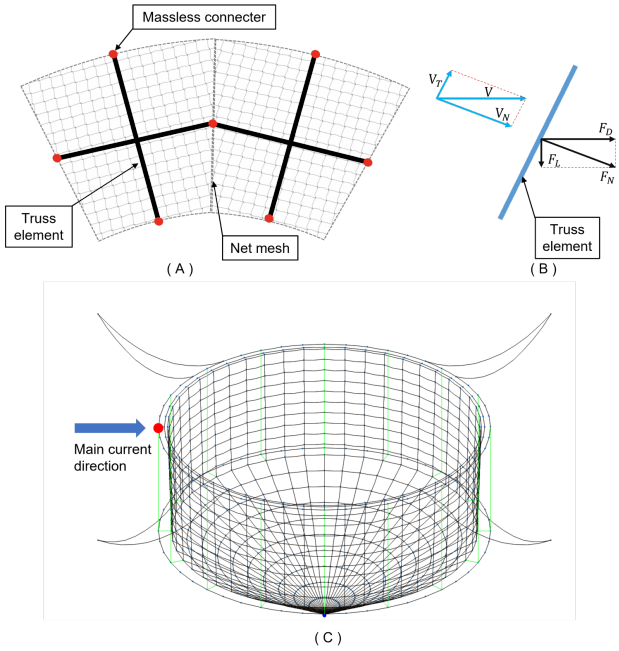

Fig. 3: Modeling the net cage: (A) Truss elements were used to represent the actual net strands. (B) The drag forces acting on the net were calculated based on Morison's equation. (C) A numerical model of a net cage in Orcaflex, with the most upstream node on the floating ring represented by the red spot.

as shown in Fig. 3. The equivalent structure element was assigned proper physical properties so that the projected area, submerge weight, and elasticity were equal to the sum of its corresponding strands. Additional details can be found in [11].

The drag term of Morison's equation was employed to determine the current loads acting on the net cage. The incident flow velocity (V) was analyzed by breaking it down into directions parallel (V_T) and normal (V_N) to the element, following the cross-flow principle. The frictional force in the tangential direction was minor compared to the normal force component (F_N) and was therefore disregarded. Consistent with [11], the Cd value for the net in the simulations was set to 1.2. The downstream portion of the net cage experiences a reduced flow velocity due to the upstream net's shielding effects. To account for this phenomenon, the downstream net was subjected to a lower flow velocity equivalent to 0.8 of the upstream flow velocity.

The floating rings and sink ring of the cage were modeled using the beam elements. The bending stiffness of the rings was determined by their cross-section properties and materials. The current forces on the rings were calculated using Morison's equation with a Cd of 1.5.

The displacement of nodes in the cage model results from two factors: the holistic movement of the cage and the local deformation. The holistic movement is in the horizontal direction and can be approximated as the displacement of

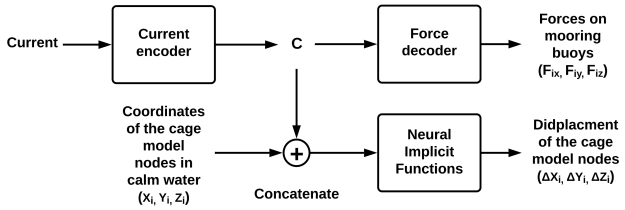

Fig. 4: Architecture of the DNN.

the node on the floating ring the most upstream to incoming currents. (Fig. 3 C) By subtracting the cage's movement components from the total displacement of each node, we can calculate the displacement of each node due to cage deformation and gain a more detailed understanding of the factors contributing to node displacement in the cage model.

C. Establishing the DNN model for fast simulation

The DNN was established using the Pytorch library. Fig. 4 shows the DNN architecture designed to predict the displacement of the cage and forces on mooring buoys in response to specific current conditions. The model consists of a Current encoder, a Force decoder, and a Neural Implicit Function (NIF).

The current encoder is used to encode the raw current data into a contextual vector c. The contextual vector c will be used by the Force decoder to predict the forces and the neural implicit function for the displacements. A simple feed-forward neural network consisting of two fully connected layers with a hidden size of 128 is used as the current encoder. The dimension of the contextual vector c is 128.

The force decoder is used to predict the force F_x, F_y, F_z on the four mooring buoys from the contextual vector c. A feed-forward neural network consisting of two fully connected layers with a hidden size of 128 is used. The output of the force decoder is a 12-dimensional vector representing the forces on the four mooring buoys.

The displacements of each node of the cage are predicted by a feed-forward neural network as well. However, in order to predict the displacements of the large numbers of nodes of the cage, the model is learned in the function space and it is sometimes called the neural implicit function in the literature. The network takes the contextual vector c and the initial coordinates x, y, z of each node of the cage model as inputs. The output is the displacements of the node $\triangle x, \triangle y, \triangle z$. Note that for a specific node of the cage, contextual vector c may vary but the initial coordinates x, y, z are fixed. The feed-forward neural network for the neural implicit function is slightly deeper and consists of four fully connected layers with a hidden size of 256.

The rectified linear unit (ReLU) activation function is used in all three components (current encoder, force decoder, neural implicit function) to introduce nonlinearity into the model.

The loss function used for training is a mean squared error (MSE) as the sum up of Eq. 1 and Eq. 2.

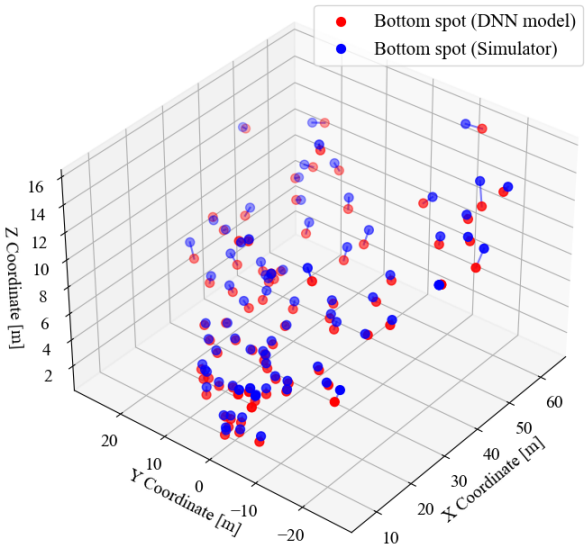

Fig. 5: Spatial distribution of the net's bottom point. Blue dots represent the simulation results, while red dots represent the results predicted by the DNN model. A straight line connects the corresponding spots.

$$L_1 = \frac{1}{N_1}\sum_{i=1}^{N_1}(X_i - \hat{X}_i)^2 + (Y_i - \hat{Y}_i)^2 + (Z_i - \hat{Z}_i)^2 \quad (1)$$

In Eq. 1, N_1 represents the total number of the nodes of the cage structures in the model, X_i, Y_i, Z_i represent the 3D coordinates of node i of simulations, $\hat{X}_i, \hat{Y}_i, \hat{Z}_i$ represent the 3D coordinates of node i of DNN model predictions.

$$L_2 = \frac{1}{N_2}\sum_{i=1}^{N_2}(F_{ix} - \hat{F_{ix}})^2 + (F_{iy} - \hat{F_{iy}})^2 + (F_{iz} - \hat{F_{iz}})^2 \quad (2)$$

In Eq. 2, N_2 represents the total number of the mooring buoys in the model, F_{ix}, F_{iy}, F_{iz} represent the components of forces on the mooring buoy i of simulations, $\hat{F_{ix}}, \hat{F_{iy}}, \hat{F_{iz}}$ represent the components of forces on the mooring buoy i of DNN model predictions.

The model is trained on a dataset of current profiles and corresponding displacement and force values with the ADAM optimizer, using a batch size of 32 and a learning rate of 0.001. The performance of the model is evaluated on a separate test set by calculating the Euclidean distance error and force error.

III. Results and Discussions

To evaluate the level of deformation experienced by the fish cage, the lifting of the bottom point of the cage was used as an indicator. Among the 90 evaluation cases, 31 cases had a lifting of the bottom point ranging from 0-5 m and were defined as cases with small deformation. Another 43 cases had a lifting ranging from 5-10 m and were defined as

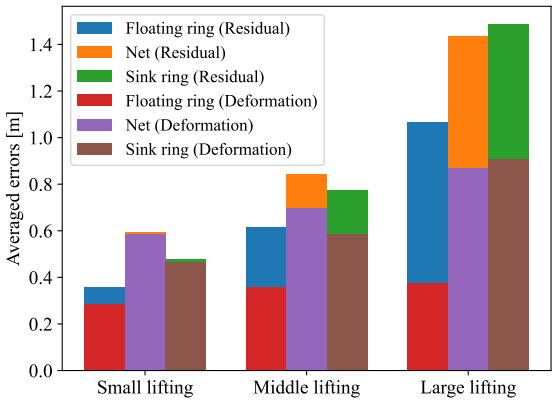

Fig. 6: The averaged deviations of the net cage between the simulation results and predictions from the DNN model. The deviations due to the discrepancy of cage deformations are compared with the total deviations.

cases with middle deformation. The remaining 16 cases had a lifting larger than 10 m and were considered cases with large deformation.

Fig. 5 displays the spatial distribution of the bottom point of the net for all 90 evaluation cases based on simulation results and DNN model predictions. The analysis reveals that the bottom points are clustered in a fan-shaped region, with their elevation correlated to the horizontal displacement, which aligns with the main current direction. The horizontal displacement along the main current varies from 5 m to 60 m, whereas the displacement normal to the main current ranges from -20 m to 20 m. The relatively large horizontal displacement is primarily attributed to using a 'soft' mooring system, which aims to evaluate the DNN model's ability to handle extreme scenarios. The lifting of the bottom spot of the net ranges from 1.3 m to 15.5 m, with the largest deformation corresponding to a lifting of the bottom point to half its depth in calm water. It should be noted that significant deformation can be mitigated in real-life by adding more weights to the ballast system. The comparison of deviations between the spot positions from simulations and predictions of the DNN model indicates that the absolute error (length of the bar between the two dots) increases with cage deformation. In the group with large deformations, prediction quality is less stable.

Our results, shown in Fig. 6, indicate the MSE of the position of the cage structure nodes resulting from these two components. The DNN model was the most effective in predicting the displacement of the floating ring, while the predictions for the net and sink rings were similarly accurate but not as good as those for the floating ring. The absolute errors increased as the cage deformation increased. The errors resulting from the local deformation component remained constant with increasing deformation, while the errors resulting from the holistic movement of the cage showed a strong correlation with the level of deformation.

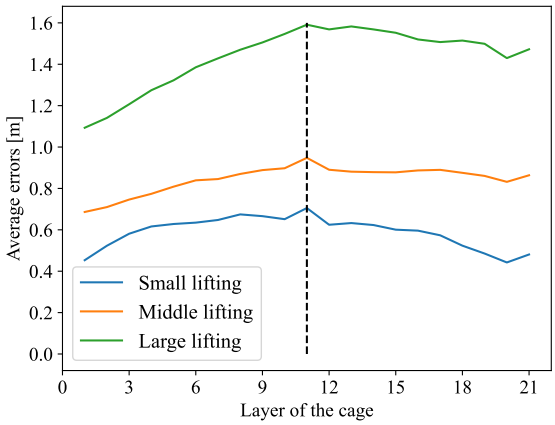

Fig. 7: The averaged deviations of the net over its vertical layers. The left side of the line of dashes (layers 1st to 10th) belongs to the cylindrical part of the cage. The right side belongs to the conic bottom of the cage

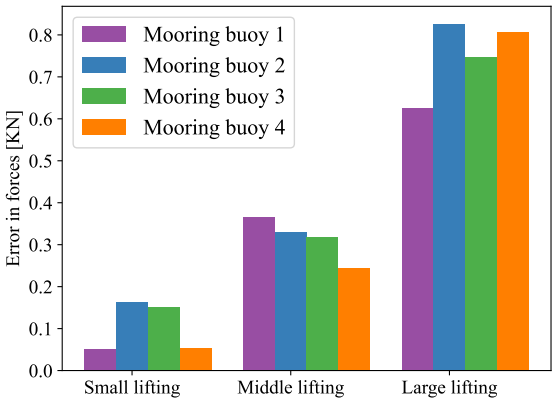

Fig. 8: The averaged deviations of the forces on the four mooring buoys between the simulation results and predictions from the DNN model.

The results shown in Fig. 7 demonstrate the MSE of the positions of nodes on different layers of the net in the cage model. The cage model consists of 20 vertically stacked layers, with 10 layers constituting the net wall and the remaining layers constituting the net bottom. The results indicate that for all deformation groups, the discrepancy in the positions of the nodes increases with depth to varying degrees, reaching a maximum at the junction between the net wall and bottom. The discrepancy then decreases slightly with further depth on the net bottom.

Fig. 8 illustrates the absolute discrepancy of forces on the four mooring buoys in the cage model. The results indicate that the relative positions of the buoys with respect to the main current do not significantly affect the accuracy of the predictions. The relative errors of the force prediction in the large lifting group are less than 10%, within the acceptable range.

Three samples selected from 90 test samples with increasing deformation were used to demonstrate a hypothetical scenario where a net cage is exposed to increasing incoming currents. The current profiles are shown in the top row of Fig. 9. The current velocity varies every 5 m from 2.5 m to 27.5 m in depth (the current velocity within the top 2.5 m is assumed to be constant), consistent with measurements obtained from an ADCP with a cell size of 5 m and without overlapping between cells. The second row of Fig. 9 shows the predicted location and shape of the cage from both the simulator and the DNN model, corresponding to the current profile shown above. Despite some local discrepancies, the DNN model is capable of providing predictions that are comparable to those of the simulator, even in areas with abrupt changes in shape, such as the upstream part of the net bottom.

One of the key advantages of the DNN model is its computational efficiency and robustness. Compared to the simulator, which requires an average of about 1.2 minutes per case on a laptop with 8*i7-10875H CPUs, the DNN model can make predictions in real-time, with an average time cost of about 0.1 seconds. When applied in a digital prototype of a fish cage, the DNN model provides the ability to make near-instant updates on cage behavior as soon as updated current information becomes available (typically every 5-10 minutes). This is in contrast to the simulator, which requires a processing time of about 1.2 minutes for each prediction. The DNN model has the added advantage of avoiding the risk of non-convergence in numerical simulations. Net cages, as flexible structures with numerous nodes, can present challenges in obtaining converged results when exposed to currents that vary in depth. In this study, 56 of the 390 total samples applied were not able to converge within 450 iteration steps during a batch simulation. This required subsequent adjustments to the simulation settings to obtain successful simulations. In a digital prototype application, the failure of a simulation can result in the absence of the desired information for the client. The DNN model provides a reliable alternative for predicting the behavior of cage structures.

Additionally, the DNN model brings several other benefits. Unlike a traditional simulator, the DNN model does not require high computational power or a specific operating system, such as Windows or MacOS, making it more flexible for integration with hardware systems. For instance, the Raspberry Pi, a low-cost, portable, and low-power consumption platform, has been used to perform light tasks. The DNN model can be run on the Raspberry Pi platform, whereas a traditional simulator may not be able to run on this platform. Furthermore, the DNN model can be a suitable form of delivery from a digital prototype maker to clients, as it avoids potential issues related to software licenses and intellectual property rights. These benefits make the DNN model a more accessible and versatile solution for predicting the behavior of cages in real-world applications.

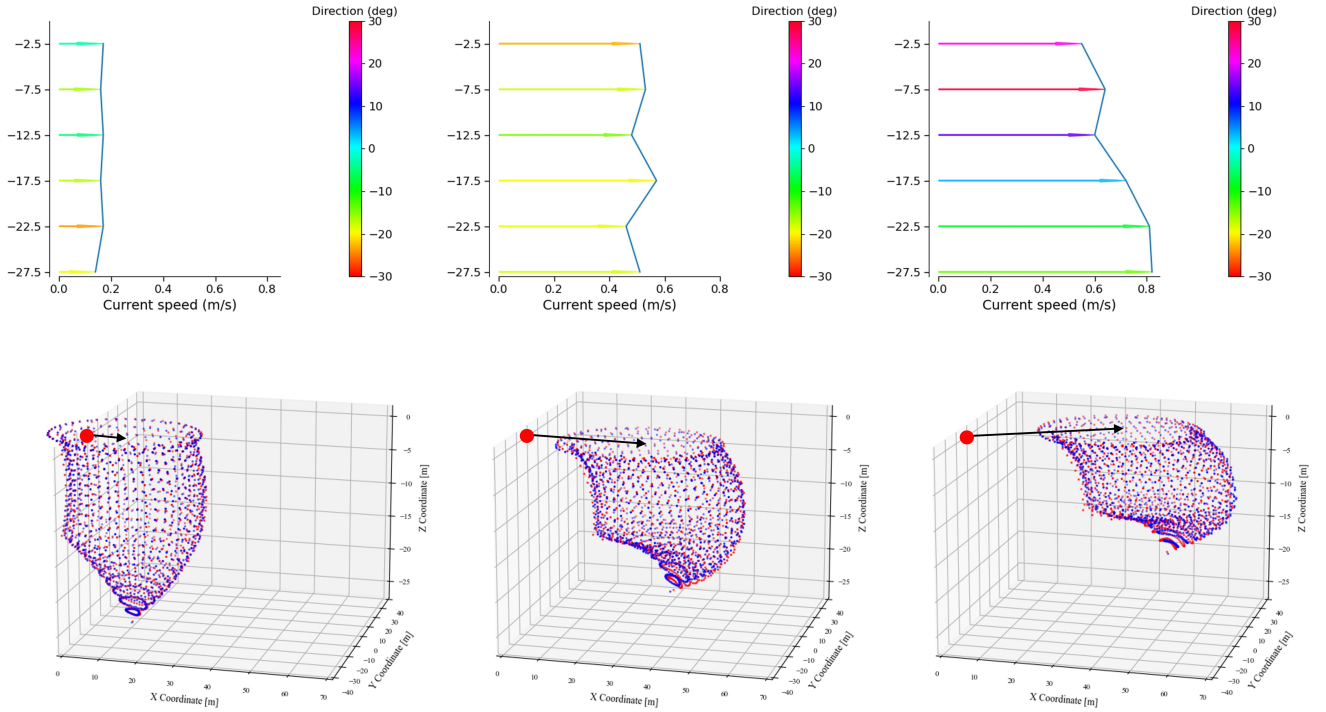

Fig. 9: A hypothetical case where the net cage is subject to an increasing current velocity. The cage shapes from the simulator are represented by blue dots, and the ones predicted by the DNN model are by red dots. The arrow line shows the holistic movement of the cage under the currents, and the solid red spot shows the original position of the cage center.

IV. CONCLUSIONS

In this study, we propose a DNN model to predict the behavior of fish cage structures in response to incoming currents. Our results show that the DNN model can provide predictions comparable to those of the simulator, with improved computational efficiency and robustness. The DNN model has an average time cost of about 0.1 seconds, compared to an average of about 1.2 minutes for the simulator, and is less susceptible to non-convergence. Furthermore, the DNN model brings several additional benefits, including its flexibility for integration with hardware systems and its suitability as a form of delivery from a digital prototype maker to clients.

In conclusion, the DNN model is a reliable and versatile solution for predicting the behavior of fish cage structures in real-world applications. By providing near-instant updates on cage behavior, the DNN model offers a valuable tool for ensuring the safety and stability of fish cage structures in challenging ocean environments.

REFERENCES

[1] T. Kristiansen and O. M. Faltinsen, "Modelling of current loads on aquaculture net cages," *Journal of Fluids and Structures*, vol. 34, pp. 218–235, 2012.

[2] P. F. Lader and A. Fredheim, "Dynamic properties of a flexible net sheet in waves and current—a numerical approach," *Aquacultural engineering*, vol. 35, no. 3, pp. 228–238, 2006.

[3] G. Rickard, "Three-dimensional hydrodynamic modelling of tidal flows interacting with aquaculture fish cages," *Journal of Fluids and Structures*, vol. 93, p. 102871, 2020.

[4] P. Klebert and B. Su, "Turbulence and flow field alterations inside a fish sea cage and its wake," *Applied Ocean Research*, vol. 98, p. 102113, 2020.

[5] H. Zhang, G. Li, L. I. Hatledal, Y. Chu, A. L. Ellefsen, P. Han, P. Major, R. Skulstad, T. Wang, and H. P. Hildre, "A digital twin of the research vessel gunnerus for lifecycle services: Outlining key technologies," *IEEE Robotics & Automation Magazine*, 2022.

[6] B. Su, K.-J. Reite, M. Føre, K. G. Aarsæther, M. O. Alver, P. C. Endresen, D. Kristiansen, J. Haugen, W. Caharija, and A. Tsarau, "A multipurpose framework for modelling and simulation of marine aquaculture systems," in *International conference on offshore mechanics and arctic engineering*, vol. 58837. American Society of Mechanical Engineers, 2019, p. V006T05A002.

[7] I. M. Holmen, T. Thorvaldsen, and K. G. Aarsæther, "Development of a simulator training platform for fish farm operations," in *International Conference on Offshore Mechanics and Arctic Engineering*, vol. 57663. American Society of Mechanical Engineers, 2017, p. V03BT02A023.

[8] S. Gao, L. C. Gansel, G. Li, and H. Zhang, "An integrated approach to modelling fish cage response in the flow," *Modeling, Identification and Control*, 2021.

[9] B. Su, E. Kelasidi, K. Frank, J. Haugen, M. Føre, and M. O. Pedersen, "An integrated approach for monitoring structural deformation of aquaculture net cages," *Ocean Engineering*, vol. 219, p. 108424, 2021.

[10] P. Han, G. Li, X. Cheng, S. Skjong, and H. Zhang, "An uncertainty-aware hybrid approach for sea state estimation using ship motion responses," *IEEE Transactions on Industrial Informatics*, vol. 18, no. 2, pp. 891–900, 2021.

[11] H. Moe, A. Fredheim, and O. S. Hopperstad, "Structural analysis of aquaculture net cages in current," *Journal of Fluids and Structures*, vol. 26, no. 3, pp. 503–516, 2010.